ACS OMEGA

Open Access



http://pubs.acs.org/journal/acsodf

Article

# Nanoliposomes for Controlled Release of Cannabinodiol at Relevant Gastrointestinal Conditions

Karol Zapata,* Stephania Rosales, As Rios, Benjamin Rojano, Jhoan Toro-Mendoza, Masoud Riazi, Camilo A. Franco, and Farid B. Cortés*

Cite This: *ACS Omega* 2023, 8, 43698−43707

Read Online

ACCESS | Metrics & More | Article Recommendations

**ABSTRACT:** Cannabidiol (CBD) has significant therapeutic potential; nevertheless, its advance as an effective drug by the pharmaceutical business is hindered by its inherent characteristics, such as low bioavailability, low water solubility, and variable pharmacokinetic profiles. This research aimed to develop nanoliposomes using an easy and low-cost method to improve the hydrosolubility of CBD and achieve a controlled delivery of the active principle under relevant physiological conditions from the mouth to the intestine; the cytotoxic and antitumor activities were also evaluated. To achieve the objective, core−shell nanoliposomes based on CBD were synthesized in three easy steps and characterized in terms of shape, size, surface chemistry, thermal capacity, and surface charge density through transmission electron microscopy (TEM), dynamic light scattering (DLS), Fourier transform infrared (FTIR), thermogravimetric analysis (TGA), and potential charge (PZ), respectively. CBD-controlled delivery trials were carried out under simulated mouth−duodenal conditions and fitted to Korsmeyer−Peppas and Noyes−Whitney models to conclude about the pharmacokinetics of CBD from nano-CBD. Cytotoxicity studies on nonmalignant human keratinocytes (HaCaT) were carried out to evaluate its safety and the recommended consumption dose, and finally, the antiproliferative capacity of nano-CBD on human colon carcinoma cells (SW480) was determined as beginning proposal for cancer treatment. The characterization results verified the water solubility for the CBD nanoencapsulated, the core−shell structure, the size in the nanometric regime, and the presence of the synthesis components. The dissolution rate at duodenal conditions was higher than that in buccal and stomach environments, respectively, and this behavior was associated with the shell (lecithin) chemical structure, which destabilizes at pH above 7.2, allowing the release by non-Fickian diffusion of CBD as corroborated by the Korsmeyer−Peppas model. In vitro biological tests revealed the innocuousness and cyto-security of nano-CBD up to 1000 mg·L$^{-1}$ when evaluated on HaCaT cells and concentrations higher than 1000 mg·L$^{-1}$ showed antitumor activity against human colon carcinoma cells (SW480) taking the first step as a chemotherapeutic proposal. These results are unprecedented and propose a selective delivery system based on nano-CBD at low cost and that provides a new form of administration and chemo treatment.

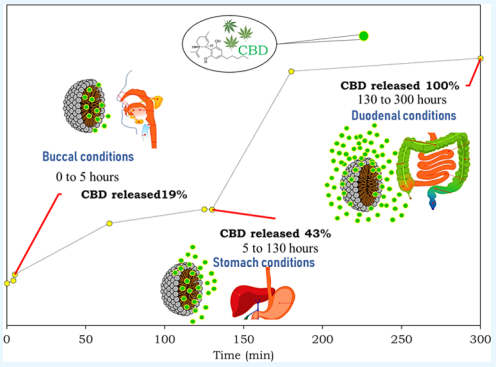


## 1. INTRODUCTION

The use of cannabis as a medicinal plant dates back to 2800 B.C., as recorded in the pharmacopoeia of the Chinese emperors prescribed to treat ailments, such as arthritis, depression, inflammation, and all kinds of pain. The use of medicinal cannabis in modern times dates back to the 19th century, when William Brooke O'Shaughnessy disseminated the first scientific results demonstrating the potential application of cannabis in patients with severe seizures, rheumatism, and cholera, providing the first conclusions about the medicinal potential of this plant without neglecting its psychotropic effects.[1] Despite the findings throughout history, it was not until 1930 that the active structures of cannabis were identified and isolated to test each of these components independently. To date, more than 400 chemical entities have been elucidated, each one with properties.[2] Approximately 60 structures known as cannabinoids have been recognized, out of which tetrahydrocannabinol (THC) and cannabidiol (CBD) stand out due to their abundance in the plant. THC is associated with psychoactive effects, while CBD is characterized by its therapeutic properties for the management of a wide spectrum of diseases. Specifically, CBD is a lipophilic and aromatic substance, whose solubility in water tends to be extremely low (0.01 mg·mL$^{-1}$), hindering direct oral consumption and dispersion in hydrophilic matrices. Its

Received: July 24, 2023
Revised: October 10, 2023
Accepted: October 19, 2023
Published: November 9, 2023

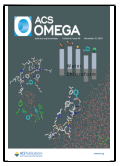

natural absorption is complex, presenting oral bioavailability values of less than 19%.[3] This condition implies the use of high doses consumed or dispersed in foods to achieve therapeutic effects. Vegetable oils have been used as carriers to improve the bioavailability of cannabinoids. Unfortunately, when they are incorporated into beverage-type consumption matrices, the affinity of the oily phase for the polymers that make up the containers is high, reducing the effective intake of CBD, making the strategy inefficient. There is evidence of the oxidative instability of edible vegetable oils, favoring the attack of the CBD molecule by radical species generated in the same oil. On the other hand, traditional drugs are based on the direct delivery of the active principle, which implies a continuous consumption of the same to achieve therapeutic effects. Added to this, there is the nonspecific distribution of the drug that leads to high toxicities of the treatments. To overcome the above challenges, the use of engineered nanocarriers is on the frontline of nanomedicine. Wang et al.[4] reported the results of hybrid nanocapsules, CBD polymers (zein and whey protein), which were synthesized, characterized, and evaluated under oversimplified physiological conditions. Tabboon et al.[5] evaluated the diffusion of immobilized CBD toward a simulated salivary medium only. In this case, CBD was transported in lipid matrices with previously exposed solubility limitations. Finally, in a study performed by Fraguas-Sánchez et al.,[6] drug release in vitro studies was performed by suspending nanoparticles (5 mg·$mL^{-1}$) in phosphate-buffered saline (PBS) (pH 7.4) containing 0.5% (w·$v^{-1}$) of Tween 80 and incubated at 37 ± 0.5 °C, 100 rpm for 96 h. Noticeably, the existing protocols for obtaining suitable carriers are expensive and time-/energy-consuming. The production of CBD microcapsules proposed by Fraguas-Sánchez et al.[6] involves at least 6 h of preparation, various stages, and more different ingredients, added to the use of separation membranes, which increases production costs. Another work reported by Wang et al.[4] suggests a lyophilization step to obtain composites able to disperse in aqueous phases. The CBD hydrogels reported by Dirksen et al.[4] follow two complex stages: surfactant-assisted precipitation polymerization and CBD loading, requiring 10 expensive steps and at least 6 h of synthesis. Some studies have been published in the last year; among them, Fu et al.,[7] Kok et al.,[8] and Shilo-Benjamini et al.[9] developed liposomes using CBD as an active ingredient. Although the aforementioned studies have evolved to *in vivo* evaluations, they differ in the difficulty of liposome synthesis, the indirect costs of the bioactive product, the lack of evaluations in human-simulated gastrointestinal conditions, and the size in a strictly nanometric regime found in the present work. In these studies, more than 5 steps are carried out for liposomal synthesis, including a number of phospholipids, detergents, analytical reagents, commercial liposomes, and crystallization methods, as well as specialized equipment, evaporators, and ultrasonicators for liposomal development, achieving, in all cases, sizes greater than 100 nm.

Liposomes can be nano or microparticulate or colloidal carriers, usually 20 nm to 5 $\mu$m in diameter, which form spontaneously when certain lipids are hydrated in aqueous media.[10] However, liposome size is one of the main parameters, which determines their effectivity.[11] For example, the reduction in liposome size has also been correlated with an increased accumulation in tumor tissue. This may partly be due to the longer circulation half-life of small liposomes compared to large liposomes. In addition, small liposomes can extravasate by passive convective transport through the tumor capillaries much more easily than large liposomes. Likewise, tumor capillaries are generally more permeable than normal, achieving more immediate effects. Extravasation of liposomes is due to their size and occurs passively; the driving force behind this is the difference between intravascular hydrostatic and interstitial pressures.[12] Finally, liposomes are highly biocompatible and biodegradable, unlike other compound carriers, and they consist of an aqueous volume entrapped by one or more bilayers of natural and/or synthetic lipids. Liposomes in turn can be carriers of the broadest polarity of active molecules, either in the phospholipid bilayer, in the entrapped aqueous volume, or at the bilayer interface. Liposomes have been investigated as carriers of various pharmacologically active agents, such as antineoplastic and antimicrobial drugs, chelating agents, steroids, vaccines, and genetic material.[10] Given the background, the objective of this work is to obtain nanoliposomes (nano-CBD) using an easy and low-cost method to improve the hydrosolubility of CBD and achieve a controlled and efficient delivery of the active principle under relevant physiological conditions from the mouth to the intestine. Also, the cytotoxic and antiproliferative activities of nano-CBD were evaluated. To achieve the objective, core−shell nanoliposomes based on CBD were synthesized in three steps and characterized in terms of shape, size, surface chemistry, thermal capacity, and surface charge density through TEM, DLS, FTIR, TGA, and PZ, respectively. CBD-controlled delivery trials were carried out under simulated mouth−duodenal conditions and fitted to Korsmeyer−Peppas and Noyes−Whitney models to conclude on the pharmacokinetics of CBD from nano-CBD; also, cytotoxicity studies on HaCaT cells were carried out to evaluate its safety and the recommended consumption dose, and finally, the antiproliferative capacity of nanoliposomes on human colon carcinoma cells (SW480) was determined as a proposal for cancer treatment. Briefly, to our knowledge, the specialized literature lacks a liposome that is easily synthesized and stable over time at different temperatures and that has been evaluated in human gastrointestinal conditions.

## 2. EXPERIMENTAL SECTION

**2.1. Materials.** Ethanol with degree of purity ≥98% was provided by Sigma Brand (Sigma-Aldrich, St. Louis, MO). Soy lecithin was bought in the local market (TECNAS, Colombia), as was CBD extract (Medellin, Colombia).

**2.2. Methods.** *2.2.1. Synthesis of CBD Nanoliposomes (Nano-CBD).* Nano-CBDs were made in-house. For this, 60 mg of CBD was dissolved in 12 mL of ethanol at 100 rpm for 1 min, and then, 60 mg of lecithin was added at 100 rpm until complete homogenization was achieved. Upon completion of the mixing stage, the solutions were taken to the complexation stage at 0 °C. Subsequently, ethanol was removed by rotary evaporation using an MMRE-04 Halthen at 60 °C and vacuum until it formed a thin layer on the surfaces of the evaporator vessel that was recovered with 10 mL of deionized water. Next, the nanostructuring process was carried out at 24 000 rpm for 2 min, and then, the resulting solutions were ultrasonicated at 1 min intervals with 5 repetitions. The nanoliposomes were stored for further study and analysis.

*2.2.2. Characterization of CBD Nanoliposomes (Nano-CBD).* To determine the physical and chemical properties of the synthesized nanoliposomes, the shape, size, surface charge density, chemical composition, and thermal properties of the



https://doi.org/10.1021/acsomega.3c05371
ACS Omega 2023, 8, 43698−43707

nanostructure were determined through transmission electron microscopy (TEM)/scanning electron microscopy (SEM), hydrodynamic analysis (DLS), potential charge (PZ), Fourier transform infrared (FTIR) spectroscopy, and thermogravimetry (TGA), respectively. An FEI Tecnai F20 TEM/STEM (Ohio) was used for the TEM analysis. For this, the nanoliposomes were dispersed in deionized water at a maximum concentration of 100 mg·L$^{-1}$, the mixture was shaken by inversion and then minor aliquots were dropped on the TEM disks, and the micrographs were obtained from different visual fields. The hydrodynamic diameter was estimated using the dynamic light scattering (DLS) technique using a NanoPlus 3 Micrometrics (Atlanta) as well as the $\zeta$-potential. For the nanoliposome size and TEM, the samples were dispersed in deionized water (20 mg·L$^{-1}$) and an aliquot was taken to the quartz cell of the equipment to perform the analysis. The average hydrodynamic diameter is obtained using the Stokes−Einstein equation, which is a function of the diffusion coefficient of the particles. The pH at which the potential is neutral is considered the zero point of charge or PZC; in this case, the surface charge is zero, which implies the possible aggregation of the structures.[13] For the determination of PZC, each nanoliposome was dispersed in solutions with pHs between 1 and 14 units completed from solutions of NaOH (0.1 M) and HCl (0.01 M). Each dispersion was taken to NanoPlus 3 equipment, and its charge potential was determined. The pH vs $\zeta$-potential relationship was plotted on the abscissa and ordinate, respectively. The Fourier transform infrared (FTIR) spectroscopy analysis was carried out with a Shimadzu IRAffinity-1 FTIR spectrophotometer (Kyoto, Japan) to identify the functional groups of the synthesis components. For this, approximately 50 mg of nanoliposome was dispersed in 50 mL of distilled water and placed in a compartment of the equipment. The transmittance of the samples was then measured as a function of number length from 4000 to 4500 cm$^{-1}$ with a resolution of 2 cm$^{-1}$, and the resulting graphs were interpreted according to previous reports. Finally, the thermal profiles were determined by thermogravimetry using a Q50 thermogravimetric analyzer (TA Instruments, Inc., New Castle, DE) at a heating rate of 5 °C·min$^{-1}$ from 30 to 800 °C under a $N_2$ flow rate of 100 mL·min$^{-1}$. For SEM analysis, a LEO 435 VP (LEO Electron Microscopy Ltd., Cambridge, U.K.) was used to observe the topography and surface morphology of the liposomes. Samples were freeze-dried first on SEM stubs and analyzed for liposome shape. Finally, the stability of the liposomes was determined during 72 h at 25, 35, and 45 °C (suggested storage temperatures).

*2.2.3. In Vitro Controlled Release Assays from CBD Nanoliposomes (Nano-CBD).* To evaluate the delivery of CBD from the nanoliposome, the change in the CBD concentration was quantified by subjecting the nanostructure to sequential physiological conditions simulating the digestive process; the scenarios considered in this trial were mouth, stomach, and duodenum. Likewise, CBD calibration curves were constructed at each physiological condition using concentrations between 1 and 1000 mg·L$^{-1}$ and a Genesys 10S Thermo spectrophotometer (Texas) at 220 nm.[14] The measurements were taken for the respective calibration curves to determine the concentration of CBD released in each case.

*2.2.3.1. Buccal conditions.* To simulate oral conditions, 1 mL of human saliva (pH 7.0) was collected and kept at 37 °C. A volume of 5 mL of the bionanofluid (10 mg in 10 mL of water) was added to the biological fluid, the system was kept in constant agitation at 55 rpm to simulate the turbulence of chewing, and the CBD concentration was evaluated at times 0 and 4 min after contact.

*2.2.3.2. Stomach conditions.* Stomach conditions were simulated by preparing a 2:1 mixture of an inorganic and organic solution containing, respectively, 2.2 g of NaCl/1.1 g of $NaH_2PO_4$/1.1 g of KCl/0.3 g of $CaCl_2$/0.4 g of $NH_4Cl$/1.3 mL of HCl, and 0.43 g of glucose/0.17 g of urea/0.2 g of bovine serum albumin (BSA)/0.5 g of pepsin equivalent. The mixture was homogenized at 55 rpm, 25 °C, and the pH was adjusted to 2.0 with 1 M HCl. Then, 12 mL of the final solution was used to mix with the solution from the buccal tests; the entire experiment was kept at 37 °C and 55 rpm. Finally, the concentration of CBD released at 0, 60, and 120 min after contact was evaluated.

*2.2.3.3. Duodenal conditions.* To simulate duodenal conditions, an inorganic solution containing 3.7 g of NaCl, 1.8 g of $NaHCO_3$, 0.2 g of $KH_2PO_4$, 1.9 g of KCl, and 0.1 g of $MgCl_2$ was prepared. Once homogenized, 0.02 g of urea, 0.2 g of $CaCl_2$, and 0.2 g of BSA mixture were kept at 37 °C and 55 rpm, and the pH was adjusted to 7.4 with NaOH. Once the duodenal solution was prepared, the solution resulting from the stomach test was added to 18 mL of this, and the concentration of CBD released at 0, 60, and 120 min after contact was evaluated.

*2.2.4. Kinetics Parameters.* The release kinetics were fitted to the Korsmeyer−Peppas model according to eq 1.[15]

$$M_t/M_\infty = kt^n \quad (1)$$

where $M_t/M_\infty$ corresponds to the fraction of drug released at time $t$, $k$ is the release constant that is characteristic for the polymer−drug interactions, and $n$ is equal to the diffusion exponent, which is characteristic of the release mechanism. The goodness of fit was confirmed by calculating the correlation coefficient ($R^2$).

Second, the Noyes−Whitney model, useful to measure the dissolution process of drugs delivery in a liquid medium, was used to calculate the dissolution rate according to eq 2.[16]

$$dW/dt = D \times A \times (C - C_s)/L \quad (2)$$

where $dW/dt$ is the dissolution rate (ng·seg$^{-1}$), $A$ is the surface area of nano-CBD ($2 \times 10^{-16}$ m$^2$), $C$ is the concentration of the solid in the main dissolution medium (g·m$^{-3}$), $C_s$ is the concentration of the solid in the diffusion layer surrounding the solid (g·m$^{-3}$), $D$ is the diffusion coefficient ($4.5 \times 10^{-9}$ m$^2$·s$^{-1}$), and $L$ is the thickness of the diffusion layer ($5 \times 10^{-9}$ m).

*2.2.5. Cytotoxicity Assays.* Cytotoxicity assays were used to predict the toxicity of substances to various tissues. *In vitro* cytotoxicity testing provides a crucial means for safety assessment and screening and for ranking compounds. The MTT method or 3-(4,5-dimethylthiazol-2-yl)-2,5 diphenyltetrazolium bromide is a colorimetric assay to measure cellular metabolic activity. During the present investigation, the method described by Bahaguna et al.[16] was carried out; for this, the previously prepared bionanofluid at 10, 100, and 1000 mg·L$^{-1}$ was evaluated on the viability of nonmalignant human keratinocytes (HaCaT) at 24 and 48 h assay. Cell line used in this study, HaCaT, is a cell line that is easy to manipulate and widely reported for cytotoxic tests due to its ability to spontaneously immortalize itself by incubating it at a high temperature and a low concentration of $Ca^{2+}$ in the culture medium. In addition, they are cells that preserve the vast


https://doi.org/10.1021/acsomega.3c05371
ACS Omega 2023, 8, 43698−43707

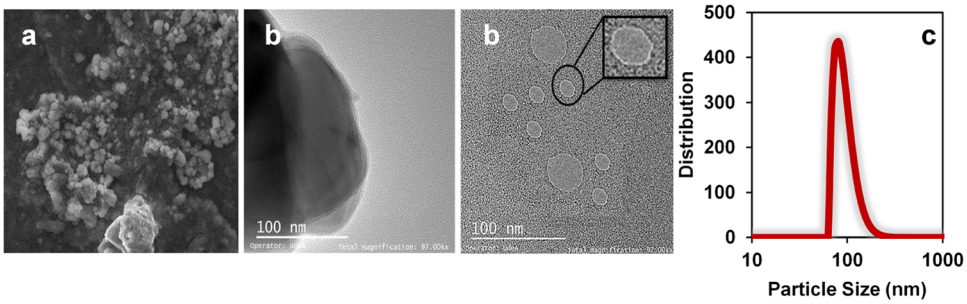


**Figure 1.** (a) Images obtained through scanning electron microscopy (SEM), (b) transmission electron microscopy (TEM), and (c) particle size distribution estimated by dynamic light scattering (DLS) for nano-CBD.

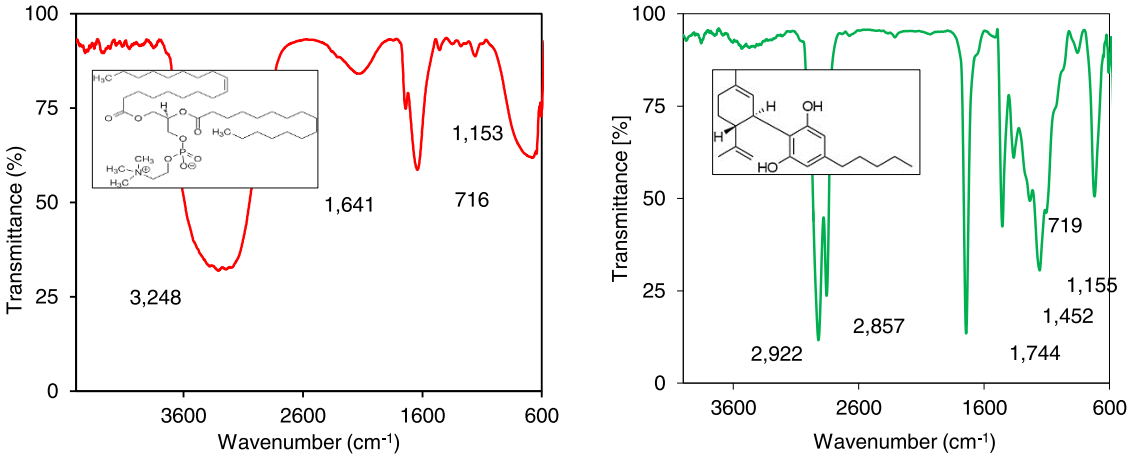


**Figure 2.** Spectra for (a) nano-CBD and (b) CBD molecules dispersed in distilled water at 25 °C using Fourier transform infrared (FTIR) spectrophotometry.

majority of the characteristics of primary human keratinocytes when manipulated in vitro.[17]

*2.2.6. Antitumor Capacity.* To evaluate the ability of CBD nanoliposomes to control cell proliferation and to be proposed as an anticancer strategy, cytotoxicity assays were performed by the MTT method according to the ISO 10993:2009 standard "Biological Evaluation of Medical Devices".[18] For this, the previously prepared bionanofluid at 10, 100, and 1000 mg·$L^{-1}$ was evaluated on the viability of human colon carcinoma cells (SW480) at 24 h assay.

## 3. RESULTS AND DISCUSSION

**3.1. Synthesis of CBD Nanoliposomes (Nano-CBD).** To verify the water solubility of the developed nanoliposomes, photographs of the suspension (1:1) were taken for 60 s. Turbidity was determined through absorbance measurements at 600 nm, as shown in Figure 1a. After 60 s, the absorbance measurement was continued every hour for 24 h, obtaining average measurements of 0.1 units and variations of less than 1%, demonstrating the stability of the suspension prepared.

The stability (absence of aggregation) is attributed to the size of the nano-CBD that improved the solvation processes according to the solubility theory (Hildebrand, 1916). For particles smaller than 1 $\mu$m, the dispersed phase exhibits a "surface", which will be covered by a "wetting surface," forming a stable chemical interface.[18] Additionally, the $\zeta$-potential for the nano-CBD at the pH of the suspension was −20 mV, representing the incidence of an anionic layer at the boundary between the nanostructure and the fluid that increases the repulsion between primary particles avoiding aggregation and subsequent sedimentation, which is like the results reported by Wang et al.[4] Lastly, both Brownian motion and low concentration are dispersing factors of nanoparticles negatively charged.

Freeze-dried samples were analyzed for liposome particle shape by SEM as shown in Figure 1a. The morphology of the nano-CBD exhibits capsule-like structures as shown in Figure 1b, and a thin layer (cover) surrounds a larger region named the core. From the mass ratio, it is expected that the core resides in the CBD molecules. According to other authors, the use of lecithin as a covering agent guarantees the formation of lipid bilayer-type liposomes by molecular arrangement.[19] Similarly, TEM images allowed testing of the nanometric regime of liposomes with sizes of less than 100 nm. The results confirmed the presence of 0D spherical particles on a nanometric scale that were irregularly agglomerated. Finally, to verify the particle size distribution, DLS measurements were performed (Figure 1c).

The size distributions present a unimodal distribution centered at 84.7 nm. These results correlate with the TEM images, confirming liposome sizes on the nanometric scale. The components of the synthesis were verified through FTIR analysis. Figure 2 presents the results for the CBD molecules and the nano-CBD. The spectrum corresponding to the nanostructure was associated with lecithin since infrared radiation directly penetrates the coverage. The peaks reported at 727 and 1641 $cm^{-1}$ were associated with vibrations of aliphatic groups $CH_2$(C−H) and $CH_3$ (C−H), and the band at 1153 $cm^{-1}$ was associated with the phosphate group ($PO_4^{3-}$), while a larger band was evidenced at 3248 $cm^{-1}$


https://doi.org/10.1021/acsomega.3c05371
ACS Omega 2023, 8, 43698−43707

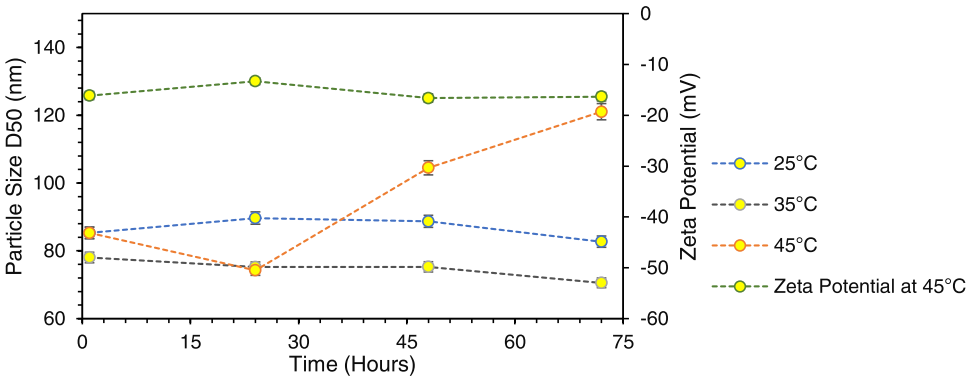


**Figure 3.** Size and $\zeta$-potential of nano-CBD stored at 25, 35, and 45 °C during 1, 24, 48, and 72 h.

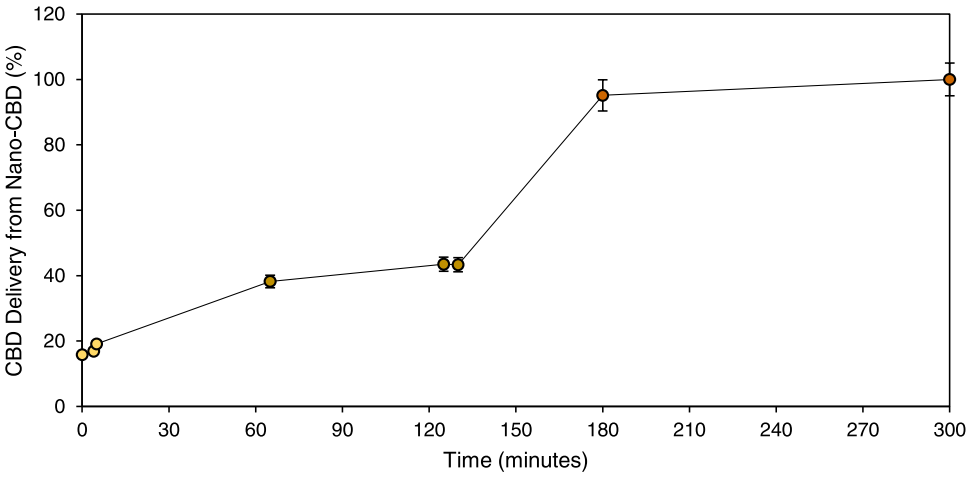


**Figure 4.** Dissolution kinetics of CBD from nano-CBD under simulated physiological conditions: Buccal (0−5 h), stomach (5−130 h), and duodenal (130−300 h) conditions. The tests were done in triplicate ($n$ = 3), and the points correspond to the mean of the measured ± standard deviation.

associated with the stretching of C═CH aliphatic groups; all of these regions are characteristic of the lecithin molecule defined as a phospholipid-like organic substance, rich in C, H, O, and P atoms.[19]

When reviewing the CBD molecule independently, it is evident that a different profile than the nano-CBD maybe due to the complete exposure of the CBD molecule to be traversed by infrared radiation: in this case, pronounced bands were recognized at 2922 and 2857 $cm^{-1}$ characteristics of the stretching of methyl ($-CH_2$) constituting aromatic rings and alkyl groups typical of the CBD molecules. Also, there were characteristic bands in 1744 and 1452 $cm^{-1}$ associated with the stretching of the C−C bond of the annular skeleton. Finally, the most important and informative bands of the aromatic compounds are found between 900 and 600 $cm^{-1}$; in the present investigation, peaks were evidenced at 1155 and 719 $cm^{-1}$ characteristics of the $C_{sp^2}$−H deformation vibrations outside of the ring plane. Other studies reveal spectra comparable to that of the present investigation.[19] The $\zeta$-potential of the nano-CBD at physiological pHs was determined. The results showed a $\zeta$-potential (mV) for nano-CBD dispersed in buffer solutions at pHs 2.1 and 7.4 simulating distribution at physiological conditions of −13.3 ± 0.65 and −16.3 ± 0.82, respectively. The intensity of the static electric field at the boundary between the nano-CBD and the fluid at the pHs evaluated was negative ($\zeta$-potential < 0) being more negative as the pH increases; with this, regardless of the evaluation condition, the particle−particle repulsion and their correct distribution in the fluid are guaranteed. This behavior is associated with the ability of the nano-CBD constituent molecules to easily deprotonate, as has been reported by other authors.[20]

Some reports have shown the instability of liposomes, especially at room temperature,[21] however, the present study demonstrated the stability of nanoliposomes for 72 h at storage temperatures from 25 °C until 45 °C as shown in Figure 3.

The stability of the suspensions is associated with the size on a nanometric scale that allows particle−solvent interaction on an atomic scale, guaranteeing thermodynamic favorability as other authors have reported.[22] On the other hand, the exposure of nanoliposomal suspensions to temperatures above 45 °C suggests an alteration evidenced through the increase in size. In parallel, the $\zeta$-potential values for that system were measured without statistical variation. The previous results allow us to conclude that the increase in size is associated with the transmembrane diffusion of water into the nanostructure without alteration in the physicochemical composition of the coating; however, in light of the results, it is possible to conclude that the display of the system for more than 72 h at 45 °C could result in the capsule breaking and releasing the contents.

**3.2. *In Vitro* Controlled Release Assays from CBD Nanoliposomes (Nano-CBD).** Figure 4 shows the release kinetics of CBD from nano-CBD under simulated physio-



https://doi.org/10.1021/acsomega.3c05371
ACS Omega 2023, 8, 43698−43707

logical conditions, and the results showed significant differences for each state ($p > 0.05$). To validate the variances, the dissolution rates were calculated using the Noyes−Whitney equation for each condition.[16] The results showed a dissolution rate according to the Noyes−Whitney equation for CBD release from nano-CBD at buccal (pH 7.4), stomach (pH 2.0), and duodenal (pH 7.4) conditions of $3.46 \times 10^{-5}$, $6.35 \times 10^{-5}$, and $8.28 \times 10^{-5}$ ng·s$^{-1}$, respectively. The dissolution rate at duodenal conditions was 2 and 1.3 times higher than that in buccal and stomach environments, respectively. Very little CBD is released in the mouth and stomach; these results are promising, considering that most of the digestion and absorption occur here when the chyme enters the duodenum.

A work carried out by Papahadjopoulos et al.[12] recommended the Noyes−Whitney model[23] to evaluate the dissolution rates of widely used drugs, such as ibuprofen and metoprolol, finding release rates at pH 4.5 and in vitro conditions of the active principles from the tablets between 3.3 × 10−15 and $5 \times 10^{-14}$ ng·s$^{-1}$, significantly slower than those found for CBD molecules from nano-CBD reported in this work. In another study reported by Hattori et al.,[16] the Noyes−Whitney model was also used to assess the rate of dissolution of theophylline. This drug is an alkaloid of the methylxanthine family, the same to which caffeine and theobromine belong, characterized by being a stimulant of the central nervous system and a bronchodilator. It is found naturally in black tea, green tea, and yerba mate. The results show an average dissolution rate of $5 \times 10^{-13}$ ng·s$^{-1}$, once again, the dissolution rate is lower than those calculated for the cannabinoid in this study. Similar results have been reported in the last 5 years for drugs, such as itraconazole,[24] entecavir,[25] and cromakalim, diproteverine HC1, and ephedrine[26] with low solubility rates on the order of mg per minute. The described results are explained by considering the virtue of nanosized carriers to increase the solubility of active principles by increasing the solute−solvent interaction at the atomic level, unlike the active principles in tablets. With respect to utilizing liposomes as vehicles for drug delivery, the success of the liposomal doxorubicin formulation (Doxil)[27] has led to the development of many other approved liposomal products. Some of the examples include Ambisome (amphotericin B),[28] DaunoXome (daunorubicin),[29] Visudyne (verteporphin),[30] Exparel (bupivacaine),[31] Marqibo (vincristine),[32] and the combination product Vyxeos (daunorubicin-cytarabine).[33] Most research into liposomes focus on the modification of the composition of the liposome bilayer and surface chemistry.[34] This includes passive, long-circulating PEGylated liposomes,[35] ligand-targeted liposomes,[36] and stimuli-responsive liposomes.[37] Despite the technological maturity of nanoencapsulated drugs for controlled release, no commercial products are obtained, or the latest studies are focused on the design of cannabinoid nanocarriers; likewise, the protocols for the preparation of nanocomposites cover various steps, increasing the complexity of the process unlike the present work.

To understand the controlled release of CBD, it is necessary to mention the lecithin chemical structure that makes up the nano-CBD shell as well as the pH of each physiological condition. Lecithin molecules are phospholipids, composed of a glycerol molecule, to which two fatty acids, 1,2-diacylglycerol, and a phosphate group, are attached. The phosphate, in turn, is linked by a phosphodiester bond to a choline molecule that is defined as a saturated quaternary amine that has a positive electrical charge.[38] The phosphate group is a triprotic system with three acidic hydrogens available to donate; a speciation diagram allowed us to verify that the predominant species at stomach pH (2.0) are completely protonated and stable (phosphoric form). However, when increasing the pH above 7.2, as occurs in duodenal conditions, deprotonated species with negative charge densities begin to predominate (monohydrogen phosphate).[39] The deprotonation of the phosphate group in the lecithin molecules favored the molecule−molecule electrostatic repulsion in the lipid bilayer of nano-CBD, allowing the relaxation of the polymer chains that constitute the shell causing the release of the active principle by non-Fickian diffusion. To verify the type of diffusion, the experimental data were fitted to the Korsmeyer−Peppas model, and this model allows us to explain drug release mechanisms, being a model generalized from the Higuchi equation.[40] It has been widely used for describing the release of drugs from polymeric systems. The "$n$" values obtained applying the Korsmeyer−Peppas model to the kinetics of CBD release from nano-CBD showed that for $n = 0$, $n = 1$, $n = 2$, and $n = 4$, the adjustment coefficient ($R^2$) was 0.691, 0.927, 0.988, and 0.999, respectively. According to the literature, a value for $n$ equal to 0.5 indicates that the drug release mechanism is of the Fickian type. It is worth mentioning that values between 0.5 and 1 indicate a non-Fickian release mechanism, while $n$ equals 1, suggesting that the mechanism is zero-order release kinetics. For values greater than 1, the drug release depends on the relaxation of the polymeric chains in the matrix, as proposed in this research according to the chemical nature of the lectin in the duodenum.[15] Few studies have evaluated the CBD diffusion parameters from carriers. However, these have not used simulated physiological media, instead have used organic solvents; in this case, the release kinetics were fitted to Fickian models, i.e., the diffusion was proportional to the CBD concentration gradient, but the structure of the capsule remains intact.[41] Nevertheless, during the present research, the CBD kinetic release was fitted to the Korsmeyer−Peppas model with $n$ greater than 1, indicating that the diffusion was entirely determined by the state of the nanocapsule shell to the intestinal condition; this conclusion is supported by the chemical nature of lecithin molecules at duodenal pH. The intestines are almost always the major site of any drug's absorption because of its specialized anatomy and much greater surface area than the stomach, so that increasing the diffusion rate of active ingredients in that area could improve the dosage and posology guidelines of the drug, increasing the therapeutic effect and reducing the adverse effects due to overdose. Although the definitions of release and absorption are not the same, the pharmacological concept of release is the first step in the absorption process, and the adequate discharge of the content of the active substance from the administered form is decisive in the adsorption parameters.[42] That is why drugs with the same dose but from different trademarks may have different bioequivalences; that is, they reach different plasmatic concentrations and, therefore, different therapeutic effects. This work approaches the development of smart nanostructures for the controlled and selective release of CBD molecules during ingestion, and the present nanostructure achieved the controlled and selective release of the CBD from nano-CBD from the mouth to the intestine and in greater proportion to duodenal conditions. There are no studies that allow comparing the release kinetics


https://doi.org/10.1021/acsomega.3c05371
ACS Omega 2023, 8, 43698−43707

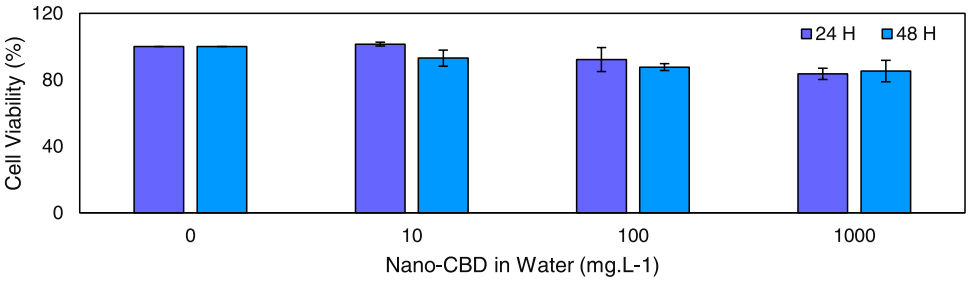


**Figure 5.** Cytotoxic activity *in vitro* of nano-CBD in water at 10, 100, and 1000 mg·L$^{-1}$ on nonmalignant human keratinocytes (HaCaT) exposed at 24 and 48 h.

of pharmaceutical forms based on CBD with the proposed nano-CBD; however, as for paracetamol—also known as acetaminophen and the most used drug worldwide for the treatment of pain—the greatest amount of active ingredient released and absorbed occurs in the proximal portion of the small intestine (the "absorption window" mainly the duodenum and jejunum).[43]

**3.3. Biological Activities for Nano-CBD.** *3.3.1. Cytotoxicity and Antitumoral Activities.* Along with the rapid growth of the nanotechnology industry comes the expansion of the number and types of manufactured nanomaterials, resulting in potentially high occupational exposures using products containing them or direct consumption of noncompounds. That is why, since the first decade of this century, there has been a growing concern about potential adverse effects on human health of exposure to nanomaterials; this concern is reflected in a growing number of scientific articles published on "nanotoxicity" or "nanotoxicology" in recent years. Many authors agree that the progressive presence in the market of products containing nanomaterials constitutes a potential emerging risk because the possible toxic effects of these nanomaterials have not yet been characterized, and many works that report the benefits of nanoproducts omit cytotoxicity tests.[44] The reduction in size provides greater bioavailability, which is accompanied by an increase in the capacity for nanomaterials to be absorbed by any biological tissue; likewise, the dimensions of the structures at atomic scales may suggest a high reactivity: living organisms are composed of cells that are usually 10−100 $\mu$m in size. However, cellular components are much smaller, and proteins, DNA, and other biomolecules are even smaller, falling within a characteristic range of 5−50 nm. This simple size comparison gives an idea that nanomaterials can be useful for accessing cellular machinery for various purposes but they can also easily interact with any cellular component to cause toxic effects. Consequently, institutions and organizations around the world, such as the US National Institute for Occupational Safety and Health, Department for Environment, Food and Rural Affairs of the United Kingdom Government, European Commission Joint Research Centre and the DECHEMA/VCI working group "Responsible Production and Use of Nanomaterials," highlight the need to increase knowledge on this topic and support nanotechnological developments with cytotoxicity assays such as those reported below.[45] Figure 5 shows the results of the cytotoxic activity of nano-CBD dispersed in water at concentrations between 10 and 1000 mg·L$^{-1}$ on nonmalignant human keratinocytes (HaCaT) at 24 and 48 h.

The results indicated that the viability of nonmalignant human keratinocytes (HaCaT) is not affected by the nano-CBD concentrations evaluated or by the exposure time up to 48 h. In addition, none of the time and concentration conditions evaluated were toxic for the cell model used, according to ISO 10993:2009, as if viability is maintained above 70%, the samples do not have cytotoxic potential.[46] The results can be explained by the chemical nature of nano-CBD. Generally, organic coatings report low reactivity thanks to the chemical stability of carbon atoms that tend to create nonpolar covalent bonds and sp3-type nonreactive chemical hybridizations.[46] For the present study, the most abundant heteroatoms in the nano-CBD were carbon, oxygen, and phosphorus, which are characterized by their low ionization energies and their poor metallic and reactive properties, suggesting less interaction with cellular components: an opposite behavior is reported by many authors for metallic nanoparticles, such as silica, aluminum, iron, zirconium, titanium, magnesium, among others, that report catalytic, magnetic, conductive, and chelating properties, among others.[47]

Instead, the antiproliferative effects were originally reported in 1975 by Munson et al.,[48] who demonstrated that delta-9-THC, delta-8-THC, and cannabinol inhibited Lewis's lung adenocarcinoma cell; likewise, other tumor cells that have been shown to be sensitive to cannabinoid-induced growth inhibition include glioma, thyroid, epithelioma, leukemia/lymphoma, neuroblastoma and skin, uterus, breast, gastric, colorectal, pancreatic, and prostate carcinomas.[49] Cannabinoids may exert their antitumor effects by several different mechanisms, including direct induction of transformed cell death, direct inhibition of transformed cell growth, and inhibition of tumor angiogenesis and metastasis. Likewise, the anticancer activity has been strongly linked to the presence of CB1 and/or CB2 receptors, i.e., the cell type. Since the late 1990s, several plant-derived (THC and CBD), synthetic (WIN-55,212-2 and HU-210) and endogenous cannabinoids (anandamide and 2-arachidonoylglycerol) have been shown to exert antiproliferative effects of a wide variety of tumor cells in cultured cancer cell lines and in mouse tumor models. To date, large volumes of literature evidence the antiproliferative and proapoptotic effects of cannabinoids on a wide variety of cancer types.[50] An evaluation of the antiproliferative activity of nanoencapsulated CBD in human colon carcinoma cells (SW480) is shown in Table 1.

After 24 h of incubation and concentrations higher than 1000 mg·L$^{-1}$, the antiproliferative power against human colon carcinoma cells (SW480) of nano-CBD is evident. A desirable property of antitumor compounds is their preferential targeting of malignant cells. There is evidence that the cannabinoids appear to kill tumor cells but do not affect their non-transformed counterparts, and may even protect them from cell death; this may explain the cytotoxic activity from 100 mg·


https://doi.org/10.1021/acsomega.3c05371
ACS Omega 2023, 8, 43698−43707

Table 1. Antitumoral Activity In Vitro of Nano-CBD in Water at 10, 100, and 1000 mg·L$^{-1}$ on Human Colon Carcinoma Cells (SW480) Exposed at 24 h

| nano-CBD concentration in water (mg·L$^{-1}$) | viability of human colon carcinoma cells (SW480) (%) |
|---|---|
| 0 | 100 |
| 10 | 100 |
| 100 | 99 |
| 1000 | 82 |
| 10 000 | 49 |

L$^{-1}$ for human colon carcinoma cells (SW480) but not for nonmalignant human keratinocytes (HaCaT) found in the present study. For example, a study by Abrams et al.[51] revealed the ability of a cannabinoid extract to induce apoptosis of glioma cells through the activation of CB1 and CB2 receptors. In contrast, cannabinoids protected normal glial cells from CB1 receptor-mediated apoptosis. Despite impressive findings *in vitro* and in animal models regarding the potential antitumor effects of cannabinoids, there is still no convincing basis for a claim that cannabinoids can "cure cancer".[52−55]

For example, increasing numbers of patients in North America are seeking oils high in THC and/or CBD due to testimonials that patients have used these preparations either topically to eradicate skin cancers or systemically to eliminate nonskin cancers.[53,56] Although the in vitro and animal evidence are intriguing, there have not yet been robust human studies investigating cannabis as an anticancer agent; however, the antiproliferative and cytotoxic evaluations at *in vitro* conditions are an unavoidable step during the discovery of new chemotherapeutic drugs. From a clinical point of view, it is necessary to carry out robust and convincing tests associated with the anticancer effects of liposomal systems. This initial approach represents an opportunity to improve and propose new strategies in the treatment of diseases such as cancer within preclinical development of how it is suggested by Food and Drug Administration (Drugs undergo laboratory and animal testing to answer basic questions about safety). These studies must be complemented with in-depth analysis of in vitro and in vivo to guarantee the safety and efficiency of liposomal systems as carriers of active components for the treatment of diseases and thus migrate to stages of clinical research and legal reviews. This study is an emerging but unavoidable stage in The Drug Development Process.[17]

The nanoliposomes developed in the present proposal had a CBD concentration of 0.1% w/w. Although the loading capacity of the nanoliposomes was not evaluated for this study, there is evidence that allows us to conclude the recommended dose of CBD for consumption. Various studies related to CBD employ different daily doses, 1−50 mg/kg for epilepsy treatment,[57] 25 mg/mL for amyotrophic lateral sclerosis treatment,[58] and between 300 and 900 mg for chronic pain treatment.[59] This heterogeneity in the concentrations used in studies demonstrates the absence of a fixed recommended CBD dosage. Due to the growing market for CBD-containing products, an authority that has addressed recommended CBD concentrations in various food and pharmaceutical products is the European Food Safety Authority (EFSA). EFSA mentions a lower confidence limit of the benchmark dose (BMDL) of 20 mg/kg of body weight/day. Furthermore, it defines the lowest observed adverse effect level (LOAEL) as 4.3 mg/kg and considers products exceeding a health-based guidance value (HBGV) of 10 mg/day to be unsafe.[60] According to the standards, the dosing of liposomes must be adjusted in accordance with the consumer product and its corresponding regulations, taking into account the concentration at which the liposomes are prepared.

The results of the present investigation preliminarily define the conditions of concentration, cell line, and time for the chemotherapeutic effect of CBD-based nanostructures. To date, there is no human study on the chemotherapeutic capacity of CBD, which represents an encouraging invitation to look for its potential use within this context.

## 4. CONCLUSIONS

The present work proposes a cost-effective protocol of elaboration of CBD hydrosoluble nanoencapsulates with excellent performance as carriers under gastrointestinal conditions. The characterization results verified the water solubility for the CBD nanoencapsulated (100%), the core−shell structure, the size in the nanometric regime (84.7 nm), and the presence of the synthesis components. The dissolution rate at duodenal conditions was 2 and 1.3 times higher than that in buccal and stomach environments, respectively; this behavior was associated with the shell (lecithin) chemical structure, which destabilizes at pH above 7.2, allowing the release by non-Fickian diffusion of CBD as corroborated by the Korsmeyer−Peppas model. In vitro biological tests revealed that innocuousness and cyto-security of nano-CBD up to 1000 mg·L$^{-1}$ when evaluated on HaCaT cells at concentrations higher than 1000 mg·L$^{-1}$ showed antitumor activity against human colon carcinoma cells (SW480) taking the first step as a chemotherapeutic proposal. Likewise, the ability of nanoliposomes to act selectively against unhealthy cells is highlighted. These results are unprecedented and propose a selective delivery system based on nano-CBD at low cost and that provides a new form of administration and chemo treatment. Results open new possibilities to overcome the technical limitations that CBD-based therapies are currently facing in terms of solubility, bioavailability, pharmacokinetics, and cyto-selective activity. From a clinical point of view, it is necessary to carry out robust and convincing tests associated with the anticancer effect of liposomal systems. This initial approach represents an opportunity to improve and propose new strategies in the treatment of diseases such as cancer within preclinical development, as suggested by the Food and Drug Administration (stage 2: drugs undergo laboratory and animal testing to answer basic questions about safety). These studies must be complemented with in-depth analysis of in vitro and in vivo to guarantee the safety and efficiency of liposomal systems as carriers of active components for the treatment of diseases and thus migrate to stages of clinical research and legal reviews. This study is an emerging but unavoidable stage in The Drug Development Process.

## AUTHOR INFORMATION

### Corresponding Authors

**Karol Zapata** − *Grupo de Investigación en Fenómenos de Superficie—Michael Polanyi, Departamento de Procesos y Energía, Facultad de Minas, Universidad Nacional de Colombia, Medellín 050034, Colombia;* orcid.org/0000-0003-0850-4556; Email: kzapata@unal.edu.co

**Farid B. Cortés** − *Grupo de Investigación en Fenómenos de Superficie—Michael Polanyi, Departamento de Procesos y Energía, Facultad de Minas, Universidad Nacional de*



https://doi.org/10.1021/acsomega.3c05371
ACS Omega 2023, 8, 43698−43707

*Colombia, Medellín 050034, Colombia;* orcid.org/0000-0003-1207-3859; Email: fbcortes@unal.edu.co

### Authors

**Stephania Rosales** − *Grupo de Investigación en Fenómenos de Superficie—Michael Polanyi, Departamento de Procesos y Energía, Facultad de Minas, Universidad Nacional de Colombia, Medellín 050034, Colombia*

**As Rios** − *Grupo de Investigación en Fenómenos de Superficie—Michael Polanyi, Departamento de Procesos y Energía, Facultad de Minas, Universidad Nacional de Colombia, Medellín 050034, Colombia*

**Benjamin Rojano** − *Grupo de Investigación Química de los Productos Naturales y los Alimentos, Escuela de Química, Facultad de Ciencias, Universidad Nacional de Colombia, Medellín 050034, Colombia*

**Jhoan Toro-Mendoza** − *Centro de Biomedicina Molecular (CBM), Laboratorio de Química Biofísica Teórica y Experimental (LQBTE), Instituto Venezolano de Investigaciones Científicas (IVIC), 4001 Maracaibo, Zulia, Venezuela;* orcid.org/0000-0003-4916-7445

**Masoud Riazi** − *Enhanced Oil Recovery Research Center, Department of Petroleum Engineering, School of Chemical and Petroleum Engineering, Shiraz University, Shiraz 36589-54268, Iran*

**Camilo A. Franco** − *Grupo de Investigación en Fenómenos de Superficie—Michael Polanyi, Departamento de Procesos y Energía, Facultad de Minas, Universidad Nacional de Colombia, Medellín 050034, Colombia;* orcid.org/0000-0002-6886-8338

Complete contact information is available at: https://pubs.acs.org/10.1021/acsomega.3c05371

### Author Contributions

K.Z., S.R., and A.R. contributed to design, conception, data acquisition, analysis, interpretation, writing—original draft preparation, and critically revised the manuscript; B.R., J.T.-M., M.R., C.A.F., and F.B.C. contributed to the conception, design, and critically revised the manuscript. All authors gave final approval and agreed to be accountable for all aspects of the work.

### Funding

"Fondo Nacional de Financiamiento Para la Ciencia, La Tecnología y La Innovación Francisco José de Caldas" provided the financial support for this project.

### Notes

The authors declare no competing financial interest.

## ■ ACKNOWLEDGMENTS

The authors specifically express our appreciation to the research group Fenómenos de Superficie "Michael Polanyi". The Universidad Nacional de Colombia jointly supports this study.

## ■ REFERENCES

(1) O'Shaughnessy, W. B. el "abuelo" de la investigación con cannabis que introdujo la marihuana en la medicina occidental hace más de 150 años. https://www.bbc.com/mundo/noticias-44128648.

(2) Richards, J. R.; Gordon, B. K.; Danielson, A. R.; Moulin, A. K. Pharmacologic Treatment of Cannabinoid Hyperemesis Syndrome: A Systematic Review. *Pharmacother. J.* **2017**, *37* (6), 725−734.

(3) Mannila, J.; Järvinen, T.; Järvinen, K.; Jarho, P. Precipitation Complexation Method Produces Cannabidiol/β-Cyclodextrin Inclusion Complex Suitable for Sublingual Administration of Cannabidiol. *J. Pharm. Sci.* **2007**, *96* (2), 312−319.

(4) Wang, C.; Cui, B.; Sun, Y.; Wang, C.; Guo, M. Preparation, Stability, Antioxidative Property and in Vitro Release of Cannabidiol (CBD) in Zein-Whey Protein Composite Nanoparticles. *LWT* **2022**, *162*, No. 113466.

(5) Tabboon, P.; Pongjanyakul, T.; Limpongsa, E.; Jaipakdee, N. In Vitro Release, Mucosal Permeation and Deposition of Cannabidiol from Liquisolid Systems: The Influence of Liquid Vehicles. *Pharmaceutics* **2022**, *14* (9), 1787.

(6) Fraguas-Sánchez, A.; Fernández-Carballido, A.; Simancas-Herbada, R.; Martin-Sabroso, C.; Torres-Suárez, A. I. CBD Loaded Microparticles as a Potential Formulation to Improve Paclitaxel and Doxorubicin-Based Chemotherapy in Breast Cancer. *Int. J. Pharm.* **2020**, *574*, No. 118916.

(7) Fu, J.; Zhang, K.; Lu, L.; Li, M.; Han, M.; Guo, Y.; Wang, X. Improved Therapeutic Efficacy of CBD with Good Tolerance in the Treatment of Breast Cancer through Nanoencapsulation and in Combination with 20 (S)-Protopanaxadiol (PPD). *Pharmaceutics* **2022**, *14* (8), 1533.

(8) Kok, L. Y.; Bannigan, P.; Sanaee, F.; Evans, J. C.; Dunne, M.; Regenold, M.; Ahmed, L.; Dubins, D.; Allen, C. Development and Pharmacokinetic Evaluation of a Self-Nanoemulsifying Drug Delivery System for the Oral Delivery of Cannabidiol. *Eur. J. Pharm. Sci.* **2022**, *168*, No. 106058.

(9) Shilo-Benjamini, Y.; Cern, A.; Zilbersheid, D.; Hod, A.; Lavy, E.; Barasch, D.; Barenholz, Y. A Case Report of Subcutaneously Injected Liposomal Cannabidiol Formulation Used as a Compassion Therapy for Pain Management in a Dog. *Front. Vet. Sci.* **2022**, *9*, No. 892306.

(10) Bangham, A. D.; Horne, R. W. Negative Staining of Phospholipids and Their Structural Modification by Surface-Active Agents as Observed in the Electron Microscope. *J. Mol. Biol.* **1964**, *8* (5), 660−IN10.

(11) Harashima, H.; Sakata, K.; Funato, K.; Kiwada, H. Enhanced Hepatic Uptake of Liposomes through Complement Activation Depending on the Size of Liposomes. *Pharm. Res.* **1994**, *11* (3), 402−406.

(12) Yuan, F.; Leunig, M.; Huang, S. K.; Berk, D. A.; Papahadjopoulos, D.; Jain, R. K. Microvascular Permeability and Interstitial Penetration of Sterically Stabilized (Stealth) Liposomes in a Human Tumor Xenograft. *Cancer Res.* **1994**, *54* (13), 3352−3356.

(13) Kosmulski, M.; Saneluta, C. Point of Zero Charge/Isoelectric Point of Exotic Oxides: Tl2O3. *J. Colloid Interface Sci.* **2004**, *280* (2), 544−545.

(14) Wang, Y.-H.; Avula, B.; ElSohly, M. A.; Radwan, M. M.; Wang, M.; Wanas, A. S.; Mehmedic, Z.; Khan, I. A. Quantitative Determination of Δ9-THC, CBG, CBD, Their Acid Precursors and Five Other Neutral Cannabinoids by UHPLC-UV-MS. *Planta Med.* **2018**, *84* (04), 260−266.

(15) Wu, I. Y.; Bala, S.; Škalko-Basnet, N.; Di Cagno, M. P. Interpreting Non-Linear Drug Diffusion Data: Utilizing Korsmeyer-Peppas Model to Study Drug Release from Liposomes. *Eur. J. Pharm. Sci.* **2019**, *138*, No. 105026.

(16) Hattori, Y.; Haruna, Y.; Otsuka, M. Dissolution Process Analysis Using Model-Free Noyes−Whitney Integral Equation. *Colloids Surf., B* **2013**, *102*, 227−231.

(17) Fusenig, N. E.; Boukamp, P. Multiple Stages and Genetic Alterations in Immortalization, Malignant Transformation, and Tumor Progression of Human Skin Keratinocytes. *Mol. Carcinog.* **1998**, *23* (3), 144−158, DOI: 10.1002/(sici)1098-2744(199811)23:33.0.co;2-u.

(18) ISO. *ISO 10993: Biological Evaluation of Medical Devices*, 2009.

(19) Bozzuto, G.; Molinari, A. Liposomes as Nanomedical Devices. *Int. J. Nanomed.* **2015**, *10*, 975.

(20) Maherani, B.; Arab-Tehrany, E.; R Mozafari, M.; Gaiani, C.; Linder, M. Liposomes: A Review of Manufacturing Techniques and Targeting Strategies. *Curr. Nanosci.* **2011**, *7* (3), 436−452.

(21) De Smet, M.; Langereis, S.; van den Bosch, S.; Grüll, H. Temperature-Sensitive Liposomes for Doxorubicin Delivery under MRI Guidance. *J. Controlled Release* **2010**, *143* (1), 120−127.
(22) Wu, L.; Zhang, J.; Watanabe, W. Physical and Chemical Stability of Drug Nanoparticles. *Adv. Drug Delivery Rev.* **2011**, *63* (6), 456−469.
(23) Lindberg, N.-O.; Lundstedt, T. The Relationship between the Dissolution Rate and the Particle Size of Prednimustine: A Disagreement with the Noyes-Whitney Equation. *Drug Dev. Ind. Pharm.* **1994**, *20* (16), 2547−2550.
(24) Sardana, K.; Khurana, A.; Panesar, S.; Singh, A. An Exploratory Pilot Analysis of the Optimal Pellet Number in 100 Mg of Itraconazole Capsule to Maximize the Surface Area to Satisfy the Noyes−Whitney Equation. *J. Dermatol. Treat.* **2021**, *32* (7), 788−794.
(25) Kang, Y.; Chen, J.; Duan, Z.; Li, Z. Predicting Dissolution of Entecavir Using the Noyes Whitney Equation. *Dissolution Technol.* **2023**, *30* (1), 38−45.
(26) Al-Janabi, I. I. An Approach for the Prediction of the Intrinsic Dissolution Rates of Drugs under Unbuffed Conditions. *Drug Dev. Ind. Pharm.* **1990**, *16* (2), 347−360.
(27) Barenholz, Y. (Chezy). Doxil — The First FDA-Approved Nano-Drug: Lessons Learned. *J. Controlled Release* **2012**, *160* (2), 117−134.
(28) Adler-Moore, J.; Proffitt, R. T. AmBisome: Liposomal Formulation, Structure, Mechanism of Action and Pre-Clinical Experience. *J. Antimicrob. Chemother.* **2002**, *49* (Suppl1), 21−30.
(29) Forssen, E. A. The Design and Development of DaunoXome for Solid Tumor Targeting in Vivo. *Adv. Drug Delivery Rev.* **1997**, *24* (2), 133−150.
(30) Verteporfin in Photodynamic Therapy Study Group. Verteporfin Therapy of Subfoveal Choroidal Neovascularization in Age-Related Macular Degeneration: Two-Year Results of a Randomized Clinical Trial Including Lesions with Occult with No Classic Choroidal Neovascularization. *Am. J. Ophthalmol.* **2001**, *131* (5), 541−560, DOI: 10.1016/s0002-9394(01)00967-9.
(31) McAlvin, J. B.; Padera, R. F.; Shankarappa, S. A.; Reznor, G.; Kwon, A. H.; Chiang, H. H.; Yang, J.; Kohane, D. S. Multivesicular Liposomal Bupivacaine at the Sciatic Nerve. *Biomaterials* **2014**, *35* (15), 4557−4564.
(32) Silverman, J. A.; Deitcher, S. R. Marqibo (Vincristine Sulfate Liposome Injection) Improves the Pharmacokinetics and Pharmacodynamics of Vincristine. *Cancer Chemother. Pharmacol.* **2013**, *71* (3), 555−564.
(33) Franco, M. S.; Oliveira, M. C. Liposomes Co-Encapsulating Anticancer Drugs in Synergistic Ratios as an Approach to Promote Increased Efficacy and Greater Safety. *Anti-Cancer Agents Med. Chem.* **2019**, *19* (1), 17−28.
(34) Torchilin, V. P. Recent Advances with Liposomes as Pharmaceutical Carriers. *Nat. Rev. Drug Discovery* **2005**, *4* (2), 145−160.
(35) Nag, O. K.; Awasthi, V. Surface Engineering of Liposomes for Stealth Behavior. *Pharmaceutics* **2013**, *5* (4), 542−569.
(36) Noble, G. T.; Stefanick, J. F.; Ashley, J. D.; Kiziltepe, T.; Bilgicer, B. Ligand-Targeted Liposome Design: Challenges and Fundamental Considerations. *Trends Biotechnol.* **2014**, *32* (1), 32−45.
(37) Movahedi, F.; Hu, R. G.; Becker, D. L.; Xu, C. Stimuli-Responsive Liposomes for the Delivery of Nucleic Acid Therapeutics. *Nanomed. Nanotechnol. Biol. Med.* **2015**, *11* (6), 1575−1584.
(38) Cui, Z.; Houweling, M. Phosphatidylcholine and Cell Death. *Biochim. Biophys. Acta* **2002**, *1585* (2−3), 87−96.
(39) Todd, B. D.; Davis, P. J. Confined Molecular Fluids. In *Nonequilibrium Molecular Dynamics*; Cambridge University Press: Cambridge, 2017; pp 294−305.
(40) Paul, D. R. Elaborations on the Higuchi Model for Drug Delivery. *Int. J. Pharm.* **2011**, *418* (1), 13−17.
(41) Moqejwa, T.; Marimuthu, T.; Kondiah, P. P. D.; Choonara, Y. E. Development of Stable Nano-Sized Transfersomes as a Rectal Colloid for Enhanced Delivery of Cannabidiol. *Pharmaceutics* **2022**, *14* (4), 703.
(42) Mora-Huertas, C. E.; Fessi, H.; Elaissari, A. Polymer-Based Nanocapsules for Drug Delivery. *Int. J. Pharm.* **2010**, *385* (1−2), 113−142.
(43) Macierzanka, A.; Rigby, N. M.; Corfield, A. P.; Wellner, N.; Böttger, F.; Mills, E. N. C.; Mackie, A. R. Adsorption of Bile Salts to Particles Allows Penetration of Intestinal Mucus. *Soft Matter* **2011**, *7* (18), 8077−8084.
(44) Seaton, A.; Tran, L.; Aitken, R.; Donaldson, K. Nanoparticles, Human Health Hazard and Regulation. *J. R. Soc. Interface* **2010**, *7* (suppl_1), S119−S129.
(45) NanoKommission of the German Federal Government. *Responsible Use of Nanotechnologies: Report and Recommendations of the German Federal Goverment's NanoKommission for 2008*, 2008.
(46) Bulbule, A. M.; Mandroli, P. S.; Bhat, K. G.; Bogar, C. M. In Vitro Evaluation of Cytotoxicity of Emblica Officinalis (Amla) on Cultured Human Primary Dental Pulp Fibroblasts. *J. Indian Soc. Pedod. Prev. Dent.* **2019**, *37* (3), 251.
(47) Blackman, J. *Metallic Nanoparticles*; Elsevier, 2008.
(48) Jia, W.; Hegde, V. L.; Singh, N. P.; Sisco, D.; Grant, S.; Nagarkatti, M.; Nagarkatti, P. S. Δ9-Tetrahydrocannabinol-Induced Apoptosis in Jurkat Leukemia T Cells Is Regulated by Translocation of Bad to Mitochondria. *Mol. Cancer Res.* **2006**, *4* (8), 549−562.
(49) Munson, A. E.; Harris, L. S.; Friedman, M. A.; Dewey, W. L.; Carchman, R. A. Antineoplastic Activity of Cannabinoids. *J. Natl. Cancer Inst.* **1975**, *55* (3), 597−602.
(50) Seltzer, E. S.; Watters, A. K.; MacKenzie, D., Jr; Granat, L. M.; Zhang, D. Cannabidiol (CBD) as a Promising Anti-Cancer Drug. *Cancers* **2020**, *12* (11), 3203.
(51) Abrams, D. I.; Guzman, M. Cannabis in Cancer Care. *Clin. Pharmacol. Ther.* **2015**, *97* (6), 575−586.
(52) Henry, J. G.; Shoemaker, G.; Prieto, J. M.; Hannon, M. B.; Wakshlag, J. J. The Effect of Cannabidiol on Canine Neoplastic Cell Proliferation and Mitogen-Activated Protein Kinase Activation during Autophagy and Apoptosis. *Vet. Comp. Oncol.* **2021**, *19* (2), 253−265.
(53) Ramer, R.; Wendt, F.; Wittig, F.; Schäfer, M.; Boeckmann, L.; Emmert, S.; Hinz, B. Impact of Cannabinoid Compounds on Skin Cancer. *Cancers* **2022**, *14* (7), 1769 DOI: 10.3390/cancers14071769.
(54) de Mendonça Lima, T.; de, M.; Santiago, N. R.; Alves, E. C. R.; Chaves, D. S.; de, A.; Visacri, M. B. Use of Cannabis in the Treatment of Animals: A Systematic Review of Randomized Clinical Trials. *Anim. Health Res. Rev.* **2022**, *23* (1), 25−38.
(55) Sakarin, S.; Meesiripan, N.; Sangrajrang, S.; Suwanpidokkul, N.; Prayakprom, P.; Bodhibukkana, C.; Khaowroongrueng, V.; Suriyachan, K.; Thanasittichai, S.; Srisubat, A.; et al. Antitumor Effects of Cannabinoids in Human Pancreatic Ductal Adenocarcinoma Cell Line (Capan-2)-Derived Xenograft Mouse Model. *Front. Vet. Sci.* **2022**, *9*, No. 867575, DOI: 10.3389/fvets.2022.867575.
(56) Hinz, B.; Ramer, R. Cannabinoids as Anticancer Drugs: Current Status of Preclinical Research. *Br. J. Cancer* **2022**, *127* (1), 1−13.
(57) Pamplona, F. A.; Da Silva, L. R.; Coan, A. C. Potential Clinical Benefits of CBD-Rich Cannabis Extracts over Purified CBD in Treatment-Resistant Epilepsy: Observational Data Meta-Analysis. *Front. Neurol.* **2018**, *9*, 759.
(58) Meyer, T.; Funke, A.; Münch, C.; Kettemann, D.; Maier, A.; Walter, B.; Thomas, A.; Spittel, S. Real World Experience of Patients with Amyotrophic Lateral Sclerosis (ALS) in the Treatment of Spasticity Using Tetrahydrocannabinol: Cannabidiol (THC: CBD). *BMC Neurol.* **2019**, *19*, 222.
(59) Urits, I.; Gress, K.; Charipova, K.; Habib, K.; Lee, D.; Lee, C.; Jung, J. W.; Kassem, H.; Cornett, E.; Paladini, A.; et al. Use of Cannabidiol (CBD) for the Treatment of Chronic Pain. *Best Pract. Res. Clin. Anaesthesiol.* **2020**, *34* (3), 463−477.
(60) Lachenmeier, D. W.; Sproll, C.; Golombek, P.; Walch, S. G. Does Cannabidiol (CBD) in Food Supplements Pose a Serious Health Risk? Consequences of the EFSA Clock Stop Regarding Novel Food Authorisation. *Psychoactives* **2023**, *2*, 66−75, DOI: 10.3390/psychoactives2010005.


https://doi.org/10.1021/acsomega.3c05371
*ACS Omega* 2023, 8, 43698−43707